Nonlinear analysis of Coulomb relaxation of anisotropic distributions

H. Schamel, H. Hamnén, D. F. Düchs, and T. E. StringerM. R. O'Brien

Citation: Physics of Fluids B: Plasma Physics **1**, 76 (1989); doi: 10.1063/1.859108
View online: http://dx.doi.org/10.1063/1.859108
View Table of Contents: http://aip.scitation.org/toc/pfb/1/1
Published by the American Institute of Physics

Nonlinear analysis of Coulomb relaxation of anisotropic distributions

H. Schamel,[a] H. Hamnén,[b] D. F. Düchs, and T. E. Stringer
JET Joint Undertaking, Abingdon, Oxon, OX14 3EA, United Kingdom
M. R. O'Brien
Culham Laboratory, Abingdon, Oxon, OX14 3DB, United Kingdom

(Received 4 February 1988; accepted 21 September 1988)

The bi-Maxwellian model is employed to study the time evolution of anisotropic distributions resulting from Coulomb collisions. The rate of change of temperatures caused by like-particle collisions is described by a single ordinary differential equation for ε, where $\varepsilon = T_\perp / T_\parallel$. It exhibits a logarithmic singularity in the limit $\varepsilon \to 0$, expressing the velocity space geometry and nonlinearity in the collision operator. The temporal relaxation is compared with a numerical solution of the nonlinear Fokker–Planck equation and is found to be insensitive to changes in the collision operator in the case of $\varepsilon > 1$. For $\varepsilon < 1$, however, the relaxation toward thermal equilibrium turns out to be dependent on the chosen model. The influence of unlike-particle collisions is also investigated.

I. INTRODUCTION

Anisotropic distributions are common in fusion and space plasmas. In fusion research, for example, in tokamak devices, they are generated in the discharge by the action of the induction electric field as, for example, in runaway and slideaway regimes and/or they are produced by the auxiliary methods for supplementary heating and current drive.[1] In space physics, anisotropic distributions are frequently found, as well as, for example, in the solar wind[2] where they are caused by the mirror forces of the diverging, interplanetary magnetic field. Representing nonequilibrium states, these distributions are known to affect other dependent processes in the plasma such as the plasma transport or wave–particle interactions, and, of special importance for fusion, the fusion reactivity. The absorption of rf waves and high energy particle losses are further important examples. It is therefore desirable to learn more about its temporal behavior, which reflects the competition between the various distorting forces and the restoring Coulomb collisions.

Analytically, research on Coulomb collisions has focused mainly on situations in which the distortion from isotropic Maxwellian is weak and hence allows a perturbative linearized treatment. A survey of these studies is given in several books and reviews.[3–7] With increasing power available in fusion applications, however, the plasma is often found to be distorted so strongly that it can no longer be treated as close to thermal equilibrium and a more general discussion of the effects of anisotropy is called for.

The present paper is devoted to this latter aspect by investigating a part of this general nonequilibrium problem, namely, the relaxation of an anisotropic distribution function as a result of binary collisions. Based on partially known equations,[8–11] the time evolution of the parallel and perpendicular mean energy of a bi-Maxwellian constituent is explored in the nonlinear regime.

The paper is organized as follows: In Sec. II, we summarize the Fokker–Planck description of Coulomb relaxation based on the aforementioned weak distortion from an isotropic Maxwellian, adopting the formulation by Hinton.[7] This will serve as a reference for our nonlinear study. In Sec. III the energy relaxation resulting from like-particle collisions is studied within the class of bi-Maxwellians. It is found that the dynamics is governed by a single ordinary differential equation for $\varepsilon(\tau)$, where $\varepsilon = T_\perp / T_\parallel$ is the anisotropy parameter and τ is a normalized time. Its solution shows that the temporal evolution exhibits a singular behavior in both limits, $\varepsilon \to \infty$ and $\varepsilon \to 0$.

Whereas the former is merely a consequence of the definition of ε, occurring in a linearized treatment as well, the latter expresses both the nonlinearity of the Fokker–Planck operator and the extremity in the velocity space geometry. This latter statement is supported by the investigation of Sec. IV, where the collisional drag is calculated for a different anisotropic distribution, namely, the water bag distribution on an ellipsoidal velocity space volume, making use of potential theory. An enhancement of the drag resulting from anisotropy is generally found, becoming singular in the limit $\varepsilon \to 0$ in the same manner as $d\varepsilon/d\tau$. Section V is devoted to a linearized test-particle treatment of the relaxation of $T_\parallel$ and $T_\perp$ because of self-collisions within the bi-Maxwellian model. The essential outcome of this section is that the "parallel" relaxation, $\varepsilon < 1$, but *not* the "perpendicular" relaxation, $\varepsilon > 1$, is affected by this modification in the collision operator. What is responsible for this sensitive dependence on the collision operator is "the more one-dimensional geometry" in the former case, whereas the later relaxation process, because of its two-dimensional character, appears to be more independent of the choice of the collision operator. The question of how well the bi-Maxwellian ansatz is maintained during the relaxation is followed numerically in Sec. VI by

---

[a] Permanent address: Physikalisches Institut, Universität Bayreuth, D-8580 Bayreuth, Federal Republic of Germany.
[b] Permanent address: Institute of Electromagnetic Field Theory, Chalmers University of Technology, S-41296 Gothenburg, Sweden.

 0899-8221/89/010076-11$01.90

solving the full nonlinear Fokker–Planck equation. The result is not very surprising. Whereas the energy relaxation is fairly accurately modeled by the bi-Maxwellian model in cases when $\varepsilon > 1$, distortions from the bi-Maxwellian developing in time can no longer be ignored in cases when $\varepsilon < 1$. Finally, in Sec. VII we consider the influence of unlike-particle collisions, which have been neglected so far. Assuming, like Lehner,[9] that the unlike particles are already thermalized, a set of relaxation equations is obtained, which is analyzed qualitatively for a simple plasma, consisting of electrons and Z-fold charged ions. Only in the relaxation process of anisotropic ions is the effect of electron–ion (e–i) collisions negligible, whereas these collisions contribute in the same order as self-collisions in the case of relaxing anisotropic electrons. We present a short summary and conclusions to terminate the paper.

II. BASIC EQUATIONS AND SUMMARY OF FORMULAS VALID FOR MAXWELLIAN FIELD PARTICLES

Our starting point is the Fokker–Planck equation for small angle binary Coulomb collisions first derived by Landau,[12] according to which the time evolution of a spatially independent distribution of species a is governed by[7,12,13]

$$\partial_t f_a = -\nabla_v\cdot[\mathbf{A}_a f_a - \tfrac{1}{2}\nabla_v\cdot(\mathsf{D}_a f_a)], \tag{1}$$

where $\mathbf{A}_a$ and D_a are the dynamical friction vector and diffusion tensor, respectively. They are given by

$$\mathbf{A}_a = 2\sum_b \frac{C_{ab}}{m_a^2}\left(1+\frac{m_a}{m_b}\right)\nabla_v h_b\,, \tag{2}$$

$$\mathsf{D}_a = 2\sum_b \frac{C_{ab}}{m_a^2}\nabla_v\nabla_v g_b\,. \tag{3}$$

The summation is taken over all species, including $b=a$, which represents the effect of self-interactions. The constant C_{ab} is thereby given by

$$C_{ab} = 2\pi Z_a^2 Z_b^2 e^4 \ln\Lambda,$$

where $\ln\Lambda$ is the Coulomb logarithm and Z_b is the ionization level of a particle b.

The functions introduced in Eqs. (2) and (3) are given by

$$h_b(\mathbf{v},t) = \int d^3v'\,\frac{f_b(\mathbf{v}',t)}{|\mathbf{v}-\mathbf{v}'|}, \tag{4a}$$

$$g_b(\mathbf{v},t) = \int d^3v'\,f_b(\mathbf{v}',t)\,|\mathbf{v}-\mathbf{v}'|. \tag{4b}$$

These so-called Rosenbluth potentials are solutions of appropriate Poisson equations in velocity space, namely,

$$\nabla_v^2 h_b = -4\pi f_b, \tag{5a}$$

$$\nabla_v^2 g_b = 2h_b. \tag{5b}$$

Equations (1)–(5) are basically valid for a quiescent, nonmagnetized, uniform plasma. Kinetic equations that include collective long scale fluctuations and apply for magnetized, inhomogeneous plasmas have a considerably more elaborate form.[14–16] In certain circumstances, however, simplified versions reducing to (1) or the equivalent Landau form (see Sec. III) may be justified. Montgomery *et al.*,[17] for example, conclude that the effect of a sufficiently strong, homogeneous magnetic field is solely the replacement of the Debye length in the Coulomb logarithm by the thermal gyroradius, provided the latter is significantly greater than the mean interparticle spacing. Recent investigations[18] indicate a nonmonotonic magnetic field dependence of the Coulomb logarithm at intermediate magnetic field strength. Another type of simplification may be achieved by formulating the general (drift) kinetic equation in an appropriate action-angle coordinate space rather than in six-dimensional phase space.[19] Furthermore, strongly anisotropic distributions like the ones used in this work are potentially unstable.[20] Kinetic equations, derived so far, are generally limited by the assumption of a stable background plasma. It is common, however, to include effects of growing waves through a quasilinear-type diffusion term. Even this simplification is outside the scope of the present paper, in which, to a first approach, the feedback of these waves on the distribution function is neglected.

Coming back to our basic equation we quote another convenient form:

$$\partial_t f_a = \sum_b C_{ab}[f_a,f_b]\,, \tag{6}$$

with

$$C_{ab}[f_a,f_b] = -\Gamma_a Z_b^2 \nabla_v\cdot[(m_a/m_b)(\nabla_v h_b)f_a - \tfrac{1}{2}(\nabla_v\nabla_v g_b)\cdot\nabla_v f_a]\,, \tag{7}$$

where $\Gamma_a = 4\pi Z_a^2 e^4 \ln\Lambda\, m_a^{-2}$. Since the summation includes $b=a$, Eqs. (1) and (7), respectively, are basically nonlinear.

If, except for the considered species, all other species ($b\neq a$) are relaxed and hence can be described by isotropic Maxwellians, two major simplifications are achieved.

First, isotropy implies

$$\nabla_v h_b = h_b'(v)\hat{v}, \tag{8}$$

$$\nabla_v\nabla_v g_b = \{g_b''(v)\hat{v}\hat{v} + [g_b'(v)/v](\mathbf{1}-\hat{v}\hat{v})\}\,, \tag{9}$$

where $v=|\mathbf{v}|$, $\hat{v}$ is the unit vector in the direction of the velocity, i.e., $\hat{v}=\mathbf{v}/v$, and $\mathbf{1}$ is the unit tensor.

Second, when $f_b(v)$ is a Maxwellian,

$$f_b(v) = (n_b/v_b^3\pi^{3/2})\exp(-v^2/v_b^2), \tag{10}$$

the Rosenbluth potentials can be expressed by

$$h_b(v) = (n_b/v_b)[\Phi(Y_b)/Y_b]\,, \tag{11}$$

$$g_b(v) = n_b v_b\{(\tfrac{1}{2}+Y_b^2)[\Phi(Y_b)/Y_b] + \pi^{-1/2}\exp(-Y_b^2)\}, \tag{12}$$

where $\Phi(x) = 2/\pi^{1/2}\int_0^x dt\exp(-t^2)$ is the error function and $Y_b = v/v_b$. The density n_b and thermal velocity v_b of particle species b are defined by (10).

Splitting $\mathbf{A}_a$ and D_a into two parts, one stemming from the isotropic "field" particles ($b\neq a$), and the other one from the "self-interactions" ($b=a$), we obtain

$$\mathbf{A}_a = \mathbf{A}_a^f + \mathbf{A}_a^s\,, \tag{13}$$

$$\mathsf{D}_a = \mathsf{D}_a^f + \mathsf{D}_a^s\,, \tag{14}$$

with

$$\mathbf{A}_a^f = -\nu_a^f(v)\mathbf{v}, \tag{15}$$

$$\mathbf{A}_a^s = 2\Gamma_a Z_a^2 \nabla_v h_a(\mathbf{v}), \tag{16}$$

$$\mathsf{D}_a^f = D_{a\|}^f(v)\hat{v}\hat{v} + D_{a\perp}^f(v)(\mathbb{1} - \hat{v}\hat{v}), \tag{17}$$

$$\mathsf{D}_a^s = \Gamma_a Z_a^2 \nabla_v \nabla_v g_a(\mathbf{v}). \tag{18}$$

In Eqs. (15)–(18), ν_a^f represents the friction coefficient; $D_{a\|}^f$ and $D_{a\perp}^f$ are the parallel and perpendicular diffusion coefficient, respectively. They are a result of unlike-particle collisions.

The diffusion tensor D_a^f is diagonal in a frame in which the z axis is oriented along $\mathbf{v}$.

It is understood that the symbols $\|$ and $\perp$ in connection with the diffusion tensor refer to the direction of the particle's velocity, whereas for the other quantities introduced later they refer to a superimposed magnetic field.

Using (11) and (12) we find

$$\nu_a^f(v) = \frac{2\Gamma_a}{v}\sum_{b\neq a}\frac{n_b Z_b^2}{v_b^2}\left(1 + \frac{m_a}{m_b}\right)G\left(\frac{v}{v_b}\right), \tag{19}$$

$$D_{a\|}^f(v) = \frac{2\Gamma_a}{v}\sum_{b\neq a} n_b Z_b^2 G\left(\frac{v}{v_b}\right), \tag{20}$$

$$D_{a\perp}^f(v) = \frac{\Gamma_a}{v}\sum_{b\neq a} n_b Z_b^2\left[\Phi\left(\frac{v}{v_b}\right) - G\left(\frac{v}{v_b}\right)\right], \tag{21}$$

where $G(x) = [\Phi(x) - x\Phi'(x)]/2x^2$ is the Chandrasekhar function.

For an anisotropic, non-Maxwellian distribution f_a, $\mathbf{A}_a^s$ will generally not be parallel to $\mathbf{v}$ and D_a^s will generally not be diagonal in the $\mathbf{v}$-oriented frame. In other words, self-interactions of anisotropically distributed particles render the relaxation more complex.

In the next three sections the influence of the anisotropy on the relaxation is studied from an analytical point of view. We adopt in Sec. III a bi-Maxwellian model, in which relaxation is followed under the premises that (i) the main contribution to the collision operator comes from self-interactions, i.e., we study like-particle collisions only, and that (ii) the relaxation process takes place within the class of bi-Maxwellians.

These restrictions, which will be commented on later, are the only ones. No mutilation or restriction of the nonlinearity of the collision operator is made and any degree of anisotropy is admitted.

This model will serve as a reference later on.

III. BI-MAXWELLIAN MODEL OF NONLINEAR ENERGY RELAXATION

When self-interactions only are taken into account, the sum in Eqs. (2) and (3), respectively, reduces to one term, $b = a$, and the resulting Fokker–Planck equation written in Landau's form becomes

$$\frac{\partial}{\partial t}f(\mathbf{v},t) = \frac{\partial}{\partial \mathbf{v}}\frac{c}{m^2}\int d^3v'\left(\frac{\mathbb{1}}{u} - \frac{\mathbf{uu}}{u^3}\right)\left(\frac{\partial f(\mathbf{v},t)}{\partial \mathbf{v}}f(\mathbf{v}',t) - \frac{\partial f(\mathbf{v}',t)}{\partial \mathbf{v}'}f(\mathbf{v},t)\right), \tag{22}$$

where for convenience we have dropped the index a ($c \equiv C_{aa}$, $m \equiv m_a$) and $\mathbf{u} = \mathbf{v} - \mathbf{v}'$. A well known property of (22) is the conservation of particle number, momentum, and energy.[7] Furthermore, when there is no mean drift, the kinetic energy equals the thermal energy and we have

$$w = \int d^3v\frac{mv^2}{2}f = \int d^3v\frac{m}{2}(v_\|^2 + v_\perp^2)f = w_\| + w_\perp, \tag{23}$$

which is related to the temperatures $T_\|$ and $T_\perp$ through

$$w_\| = nT_\|/2, \quad w_\perp = nT_\perp. \tag{24}$$

The conservation of the particle number n and the energy w,

$$\dot{n} = 0 = \dot{w},$$

yields

$$\dot{T}_\perp = -\tfrac{1}{2}\dot{T}_\|. \tag{25}$$

Therefore the relaxation of the anisotropy can be described by $\dot{T}_\|$ alone.

The approach to thermal equilibrium is expressed by

$$T_\| \to T_\infty, \quad T_\perp \to T_\infty, \quad \text{as} \quad t \to \infty,$$

where T_∞ is the temperature of the final isotropic plasma. This quantity is determined by the total energy through

$$(3n/2)T_\infty = w. \tag{26}$$

In deriving $\dot{T}_\|$, the second assumption enters, namely, that f is a bi-Maxwellian,

$$f(\mathbf{v},t) = n\left(\frac{m}{2\pi}\right)^{3/2} T_\|^{-1/2} T_\perp^{-1}\exp\left[-\frac{m}{2}\left(\frac{v_\perp^2}{T_\perp} + \frac{v_\|^2}{T_\|}\right)\right], \tag{27}$$

which is assumed throughout the evolution, with time-dependent temperatures, of course.

A straightforward calculation that essentially follows Kogan[8] shows that $\dot{T}_\|$ can be expressed by two parameters: the anisotropy parameter

$$\varepsilon = T_\perp/T_\|, \tag{28}$$

and the isotropic temperature T_∞.

Normalizing the time by

$$\nu_E^{-1} = \sqrt{[m(3T_\infty)^3/\pi]}\,[1/8(Ze)^4 n \ln\Lambda], \tag{29}$$

which, apart from a factor $2/\sqrt{3}$, equals Spitzer's slowing-down time of a simple plasma,[7] we obtain

$$\frac{d\varepsilon}{d\tau} = \frac{(1+2\varepsilon)^{5/2}}{4(1-\varepsilon)}[(2+\varepsilon)g(\varepsilon) - 3], \tag{30}$$

where $\tau = \nu_E t$ and $g(\varepsilon)$ is defined by

$$g(\varepsilon) = \begin{cases}\tanh^{-1}\sqrt{1-\varepsilon}/\sqrt{1-\varepsilon}, & \varepsilon \leqslant 1,\\ \tan^{-1}\sqrt{\varepsilon - 1}/\sqrt{\varepsilon - 1}, & \varepsilon \geqslant 1.\end{cases} \tag{31}$$

Within the bi-Maxwellian model the relaxation to thermal equilibrium is therefore described by a single ordinary differential equation, given by (30).

The time scale (29) shows that the energy relaxation time of anisotropic electrons is shorter than that of Z-fold charged anisotropic ions, by a factor $(m_e/m_i)^{1/2}Z^3$, assuming quasineutrality, $n_e = Zn_i$.

The constant relaxation time is, however, only a crude representation of the isotropization time which, as we will soon see, is dependent on the strength of the anisotropy.

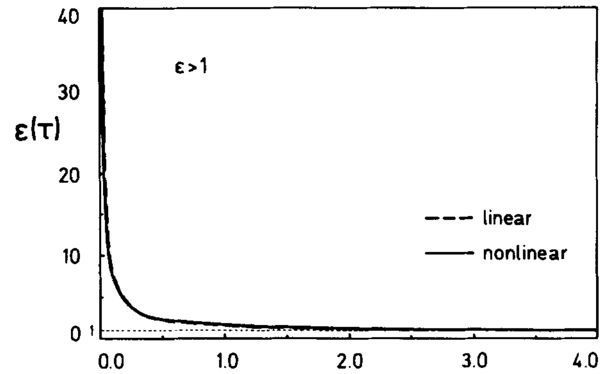

FIG. 1. The temporal evolution of the anisotropy parameter $\varepsilon = T_\perp / T_\parallel > 1$ ("perpendicular" relaxation), as a result of self-interactions. Solid line is obtained by use of the full nonlinear collision operator, whereas the dashed line refers to the test-particle approach.

The numerical solution for $\varepsilon > 1$, i.e., $T_\perp > T_\parallel$, representing the relaxation of a perpendicularly heated plasma, is shown in Fig. 1 (solid line). The ε dependence of the time scale is obvious, as is the approach to thermal equilibrium $\varepsilon = 1$. For ε going to infinity, one observes a very fast, singular-type relaxation rate. The corresponding plot for $\varepsilon < 1$, corresponding to $T_\parallel > T_\perp$, is given in Fig. 2 (solid line). Again, the ε-dependent time scale of the approach to $\varepsilon = 1$ is seen, although less pronounced.

Evaluating (30), the temporal behavior of $\varepsilon(\tau)$ can be determined explicitly for the limiting cases $\varepsilon \to 1$, $\varepsilon \to \infty$, and $\varepsilon \to 0$, respectively. For the asymptotic approach $\varepsilon \to 1$, Eq. (30) reduces to

$$\frac{d\varepsilon}{d\tau} = \frac{3^{3/2}}{5} (1 - \varepsilon), \tag{32}$$

independent of the sign of $(1 - \varepsilon)$. Defining $\delta = |\varepsilon - 1|$, Eq. (32) can be written as

$$\frac{d\delta}{d\tau} = -\frac{3^{3/2}}{5} \delta, \tag{33}$$

which has the solution

$$\delta(\tau) = \delta(0) \exp[-(3^{3/2}/5)\tau]. \tag{34}$$

The e-folding time of the energy relaxation of a weakly anisotropic plasma is therefore given exactly by

$$t^{\infty}_{\rm NL} = 5/3^{3/2}\nu_E = 10/9\nu_{\rm SP}, \tag{35}$$

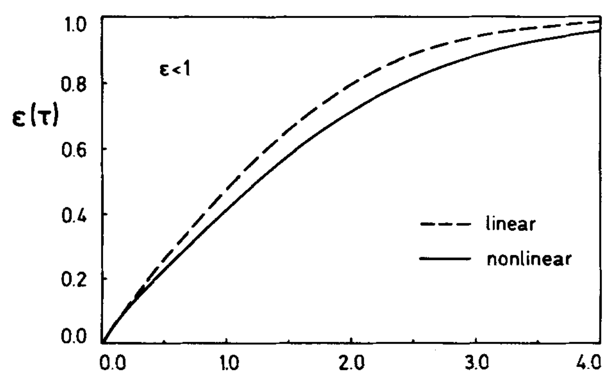

FIG. 2. Like Fig. 1, but for $\varepsilon < 1$ ("parallel" relaxation).

where $\nu_{\rm SP}$ is Spitzer's energy and momentum exchange collision frequency,[7]

$$\nu_{\rm SP} = \tfrac{4}{3}\pi^{1/2}[(Ze)^4 n \ln \Lambda / m^{1/2} T^{3/2}]. \tag{36}$$

Hence there is a slight deviation from the Spitzer time scale in the asymptotic region.

In the extreme case of very large $\varepsilon \gg 1$, Eq. (30) simplifies to

$$\frac{d\varepsilon}{d\tau} = -\frac{\pi}{\sqrt{2}} \varepsilon^2 + O(\varepsilon^{3/2}). \tag{37}$$

The solution that approaches infinity at $\tau \to 0$ becomes

$$\varepsilon(\tau) = (\sqrt{2}/\pi)(1/\tau). \tag{38}$$

As is easily seen, this singular-type nature of $\dot{\varepsilon}$ for $\varepsilon \to \infty$ is merely a consequence of the definition of ε and does not imply that the diffusion-type random walk process exhibits a singularity in this limit. It will come out in a linearized test-particle approach, as will be shown in Sec. V.

For $\varepsilon \to 0$ we obtain, by expanding (30),

$$\frac{d\varepsilon}{d\tau} = -\frac{\ln \varepsilon}{4} - \frac{1}{4}(3 - 2\ln 2) + O(\varepsilon), \tag{39}$$

which, ignoring the $O(1)$ term, is solved by

$$\varepsilon(\tau) = \exp[-E_1^{-1}(\tau/4)], \tag{40}$$

where E_1^{-1} is the inverse of the exponential integral (see, e.g., Abramowitz and Stegun[21]).

In contrast to the case $\varepsilon > 1$, the singular behavior of $\dot{\varepsilon}$ for $\varepsilon \to 0$ is a new feature in the relaxation process. It expresses the nonlinearity of the collision operator in cases where the distribution functions are extremely stretched in the parallel direction.

As we will see, this singular-type behavior is missing in a test-particle approach.

Finally, an anisotropy dependent collision frequency $\nu(\varepsilon)$ is defined by rewriting Eq. (30) as follows:

$$\frac{d\delta}{d\tau} = -\nu(\varepsilon)\delta, \tag{41}$$

where $\delta = |\varepsilon - 1|$ and $\nu(\varepsilon)$ is found to be

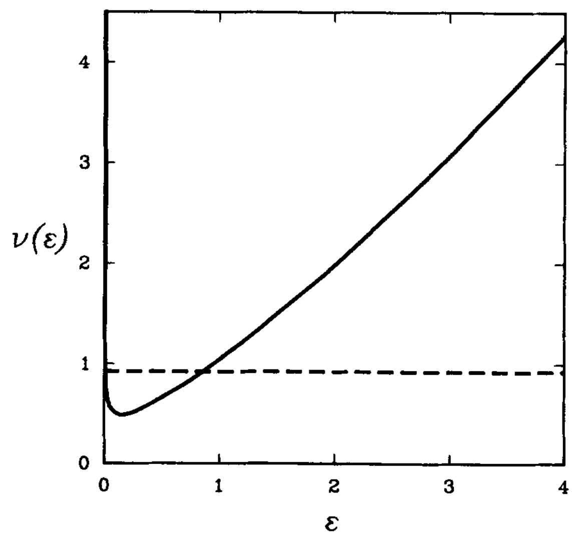

FIG. 3. The ε dependence of the energy relaxation frequency (42) in units of ν_E (29). Spitzer's constant collision frequency is given by the dashed line.

$$\nu(\varepsilon) = [(1+2\varepsilon)^{5/2}/4(1-\varepsilon)^2][(2+\varepsilon)g(\varepsilon) - 3]. \tag{42}$$

A plot of $\nu(\varepsilon)$ is drawn in Fig. 3. The dashed line represents Spitzer's collision frequency (in units of ν_E) and the time asymptotic value of ν is given by $\nu(1) = 3^{3/2}/5 = 1.04$. Again the strong dependence of the collision frequency on the anisotropy parameter is the most noteworthy feature.

IV. DRAG ENHANCEMENT BY ANISOTROPY

Next we will examine the singular behavior of $\dot{\varepsilon}$ as ε tends to zero (and the regular behavior for $\varepsilon \to \infty$, as well) from a more physical point of view. One natural suggestion is that it is the geometrical distortion of the distribution function, perhaps in combination with nonlinearity, that produces this strong enhancement of $\dot{\varepsilon}$. If this proves to be correct it should be reflected also in a similar behavior of quantities like the collisional drag.

For this reason we directly calculate the drag on a particle because of self-collisions for anisotropic distributions. To make the problem more tractable, we give up the bi-Maxwellian shape of $f(\mathbf{v})$ and replace it by a water bag distribution, keeping, however, its geometrical distortion from isotropy. According to (2) or (16) in the case of self-interactions ($b=a$) the drag or dynamical friction vector is given by

$$\mathbf{A} = (4c/m^2)\nabla_v h(\mathbf{v}), \tag{43}$$

where $h(\mathbf{v})$ is the Rosenbluth potential given by (4a) satisfying Poisson's equation (5a). (We again drop subscript a, superscript s, and ignore the time dependency in h, respectively, f.) As indicated in Sec. II there is a complete correspondence between our drag problem and electrostatics[5] given by the transformation

$$\mathbf{v}, n, f(\mathbf{v}), h(\mathbf{v}) \leftrightarrow \mathbf{x}, Q, \rho(\mathbf{x}), \phi(\mathbf{x}), \tag{44}$$

where $\rho(\mathbf{x})$ is the charge density, $\phi(\mathbf{x})$ the electrostatic potential, and Q the total charge. A drag $\mathbf{A}$ hence corresponds up to a constant to $-\mathbf{E}$, the negative of the electrostatic field.

Our goal is to obtain from a prescribed charge density $[f(\mathbf{v})]$ the electrostatic potential $[h(\mathbf{v})]$ and from there the electric field ($\mathbf{A}$). We choose an ellipsoidal charge distribution

$$\rho(\mathbf{x}) = \begin{cases} \rho_0, & \mathbf{x} \in V, \\ 0, & \mathbf{x} \notin V, \end{cases} \tag{45}$$

where

$$V = \left(\mathbf{x} \,\middle|\, \frac{x^2}{a^2} + \frac{y^2}{b^2} + \frac{z^2}{c^2} \leqslant 1\right) \tag{46}$$

and

$$a^2 \leqslant b^2 \leqslant c^2, \quad \rho_0 = Q/V.$$

The solution of the electrostatic potential problem has been found by Kellog,[22] invoking ellipsoidal coordinates. It becomes

$$\phi(\mathbf{x}) = -Ax^2 - By^2 - Cz^2 + D, \tag{47}$$

where

$$A = \pi abc\rho_0 \int_0^\infty \frac{ds}{(a^2+s)\sqrt{\chi(s)}},$$

$$D = \pi abc\rho_0 \int_0^\infty \frac{ds}{\sqrt{\chi(s)}}, \tag{48}$$

B and C being obtained from A by interchanging b with a, and c with a, respectively. The function $\chi(s)$ is given by

$$\chi(s) = (a^2+s)(b^2+s)(c^2+s). \tag{49}$$

The density ρ_0 is given by $\rho_0 = 3Q/4\pi a^2 c$.

A. The needle case (prolate spheroid)

We first discuss a charge distribution that is elongated in the (parallel) z direction and exhibits rotational symmetry about this axis ($b=a$). This configuration is a prolate spheroid and resembles for $c \gg a$ a needle with circular cross section. The electric field on the needle axis is found from (47) and is given by

$$E_z(\mathbf{x}) = 2Cz, \quad \mathbf{x} \in V, \tag{50}$$

with C given by

$$C = -\frac{3Q}{4}\left(\frac{2}{c^2(c^2-a^2)} + \frac{1}{(c^2-a^2)^{3/2}} \ln \frac{c-\sqrt{c^2-a^2}}{c+\sqrt{c^2-a^2}}\right), \tag{51}$$

valid for $c > a$. In the limit $a/c \to 0$ this expression reduces to

$$C = -(3Q/2c^3)\ln(a/c). \tag{52}$$

The electric field on the z axis therefore becomes, in this limit,

$$E_z(0,0,z) = (-3Q/c^3) z \ln(a/c), \quad |z| \leqslant c. \tag{53}$$

It is linearly dependent on z with a proportional constant becoming singular for $a/c \to 0$. Except for the origin, the electric field then becomes singular in the whole "volume" of the needle. Apart from the anisotropy, the origin of this "volume" singularity is the z dependence of the line charge density $\tau(z)$, which becomes

$$\tau(z) = \iint dx\, dy\, \rho(\mathbf{x}) = \frac{3Q}{4c}\left(1 - \frac{z^2}{c^2}\right). \tag{54}$$

If τ were constant, such as for a cylindrical constant charge distribution, a singularity would appear only in the edge region.

For comparison, we also derive the corresponding isotropic result, which is simply obtained from (50) and (51), by letting $a/c \to 1$:

$$E_z^{\text{iso}} = (Q/c^2)(z/c). \tag{55}$$

In light of the Fokker–Planck relaxation problem we thus conclude that a strong parallel anisotropy ($T_\parallel \gg T_\perp$), combined with a reduced distribution function $f(v_\parallel) = 2\pi\int dv_\perp\, v_\perp f(v_\parallel, v_\perp)$ that decreases monotonically in $v_\parallel$, gives rise to a strong friction drag for all particles, diverging in the limit $\varepsilon = T_\perp/T_\parallel \to 0$.

To make this more quantitative we define a drag enhancement factor $\alpha(\varepsilon)$ given by the quotient E_z/E_z^{iso}:

$$\alpha(\varepsilon) = \frac{-3}{(1-\varepsilon)}\left(1 + \frac{1}{2\sqrt{1-\varepsilon}} \ln \frac{1-\sqrt{1-\varepsilon}}{1+\sqrt{1-\varepsilon}}\right), \tag{56}$$

where $\varepsilon = T_\perp/T_\parallel = a^2/c^2$. A plot of $\alpha(\varepsilon)$ is given in Fig. 4.

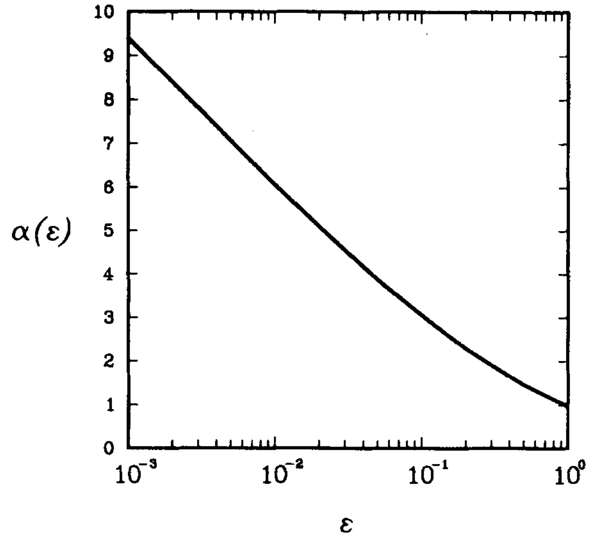

FIG. 4. The ε dependence of the drag enhancement factor α (56).

A temperature ratio of $T_\parallel/T_\perp = 10$, corresponding to $\varepsilon = 0.1$, gives an enhancement of the drag by a factor 3. The drag enhancement becomes logarithmically singular: $\alpha(\varepsilon) \approx -\frac{3}{2}\ln\varepsilon$ as $\varepsilon \to 0$. It is the same type of singularity observed in the time evolution of ε.

B. The disk case (oblate spheroid)

In the opposite limit of a perpendicularly heated plasma, the corresponding charge distribution resembles a disk or an oblate spheroid. This time we are interested in the radial electric field, which becomes

$$E_r(r,z) = 2Ar, \quad r = \sqrt{x^2+y^2}, \quad z \in V. \tag{57}$$

In contrast to the needle case, however, the constant A is now well behaved and reads

$$A = \frac{3Q}{4}\frac{1}{(a^2-c^2)}\left[\frac{-c}{a^2} + \frac{1}{\sqrt{a^2-c^2}}\left(\frac{\pi}{2} - \tan^{-1}\frac{c}{\sqrt{a^2-c^2}}\right)\right], \tag{58}$$

valid for $a > c$. In the limit of vanishing thickness ($c \to 0$), A becomes

$$A = 3\pi Q/8a^3, \tag{59}$$

and the radial electric field at $z = 0$ is given by

$$E_r(r,0) = \frac{3\pi}{4}\frac{Q}{a^2}\frac{r}{a}, \quad 0 \leqslant r \leqslant a. \tag{60}$$

It is completely regular up to the rim of the disk. Despite the zero thickness and the radial dependency of the surface charge density,

$$\sigma(r) = 2\rho_0 \int_0^{c\sqrt{1-r^2/a^2}} dz = \frac{3Q}{2\pi a^2}\sqrt{1-\frac{r^2}{a^2}}; \tag{61}$$

the resulting electric field is continuous and finite everywhere.

Singular friction forces are therefore absent in the Fokker–Planck relaxation when $T_\perp/T_\parallel \to \infty$, although a drag enhancement remains. The latter is defined by

$$\beta(\varepsilon) = E_r(r,0)/E_r^{\text{iso}}(r), \tag{62}$$

where $E_r^{\text{iso}}(r) = (Q/a^2)(r/a)$ and becomes

$$\beta(\varepsilon) = \frac{6\varepsilon^{1/2}}{(\varepsilon-1)}\left[-1 + \frac{\varepsilon}{(\varepsilon-1)^{1/2}}\left(\frac{\pi}{2} - \tan^{-1}\frac{1}{(\varepsilon-1)^{1/2}}\right)\right], \tag{63}$$

valid for $\varepsilon = T_\perp/T_\parallel = a^2/c^2 \geqslant 1$. For $c \to 0$ ($T_\parallel \to 0$) we obtain $\beta(\infty) = 3\pi/4 \approx 2.36$, i.e., no singularity occurs, and for $\varepsilon \to 1$ we have $\beta = 1$.

Similar results are expected, if the water bag ansatz for $f(v_\perp, v_\parallel)$ is relaxed and other smoother distributions, like bi-Maxwellians, are used.

These results therefore suggest that one origin for the logarithmic singularity of $\dot{\varepsilon}$ as $\varepsilon \to 0$ is the reduction to the one-dimensional velocity space geometry.

Another question is whether the nonlinearity in the collision operator is, in addition, necessary for this singular behavior. To answer this question we repeat the calculation of Sec. III but linearize the collision operator in a certain sense.

V. LINEAR TEST PARTICLE TREATMENT OF TEMPERATURE ISOTROPIZATION

As in Sec. III, we consider self-collisions only and study the relaxation within the bi-Maxwellian model. However, we modify the Coulomb collision operator by using isotropic Maxwellians in calculating the Rosenbluth potentials instead of taking the "real" bi-Maxwellian. This means the distribution is split artificially into an isotropic relaxed part that represents the "field" particles, and the rest, which is changing in time:

$$f_{\text{bM}}(v_\perp, v_\parallel, t) = f_{\text{M}}(v, T_\infty) + \delta f(v_\perp, v_\parallel, t). \tag{64}$$

This procedure in which the collision operator becomes linearly dependent on δf is called a test-particle treatment, because the particles belonging to δf interact only with field particles and not among themselves.[7]

The contribution of δf to the Rosenbluth potentials is hence ignored, and the collision operator thus obtained deviates from the correct linearized version of (7), which would read

$$C[f_{\text{M}}, \delta f] + C[\delta f, f_{\text{M}}]. \tag{65}$$

A consequence of this modification of the collision operator is that the energy is no longer conserved. In a lengthy but straightforward calculation the integrals involved in getting $dw_\parallel/dt$ and $dw_\perp/dt$ can be performed exactly.

The resulting equations read

$$\dot{x} = 3(\tfrac{3}{2})^{1/2}[1/(x-y)][(1+5x)/(1+x)^{1/2} - (1+4x+y)\sigma(x,y)], \tag{66a}$$

$$\dot{y} = -(\tfrac{3}{2})^{3/2} 1/[(x-y)\{(1+x)^{1/2}[(1+5y)/(1+y)] - (1+2x+3y)\sigma(x,y)\}, \tag{66b}$$

$$\dot{z} = 3(\tfrac{3}{2})^{1/2}[2/(1+x)^{1/2}(1+y) - \sigma(x,y)], \tag{66c}$$

where we have defined

$$x = T_\parallel/T_\infty, \quad y = T_\perp/T_\infty, \quad z = x/2 + y. \tag{67}$$

The overdot stands for $d/d\tau$ with $\tau = \nu_E t$ and $\sigma(x,y)$ is given by

$$\sigma(x,y) = \begin{cases} [1/(y-x)^{1/2}]\tan^{-1}[(y-x)/(1+x)]^{1/2}, & y \geqslant x, \\ [1/(x-y)^{1/2}]\tanh^{-1}[(x-y)/(1+x)]^{1/2}, & x \geqslant y. \end{cases} \quad (68)$$

Equation (66c), which describes the temporal charge of the total energy, is not an independent equation, but follows from (67), (66a), and (66b).

Given $\varepsilon = T_\perp / T_\parallel$, there is an arbitrariness involved in representing ε by x and y, since any common factor in x and y drops out. We remove this arbitrariness by demanding that for a given $\varepsilon_0 = \varepsilon(0)$ the initial values of x and y are chosen such that the initial energy $z_0 = z(0) = x(0)/2 + y(0) = \frac{1}{2}x_0 + y_0$ equals the final energy $z_\infty = z(\infty) = \frac{3}{2}$. Hence

$$x_0 = 3/(1+2\varepsilon_0), \quad y_0 = 3\varepsilon_0/(1+2\varepsilon_0). \quad (69)$$

With this procedure the system does not lose or gain energy globally in time, although locally the energy conservation law is violated.

The numerical solution of (66) is shown in Figs. 1 and 2 by the dashed lines.

In Fig. 1, representing $\varepsilon > 1$, the curves are almost identical, showing the relaxation is not affected by the modification of the collision operator. This changes if we consider the "parallel" relaxation, $\varepsilon < 1$ (Fig. 2). The linear relaxation now takes place faster except for very small values of ε. Particles that are more concentrated along an axis react more sensitively to a change in the effective interaction potential that is hidden in the modification of the operator.

The same conclusion can be drawn by investigating the limiting cases.

In the limit $\varepsilon \to \infty$ (i.e., $x \to 0$, $y \to \frac{3}{2}$) we find from (66)

$$\dot{x} = 1.98, \quad \dot{y} = -0.71, \quad \dot{z} = 0.28. \quad (70)$$

The energy is increasing in this limit. Approximating $\dot{\varepsilon}$ by $-\varepsilon^2 \dot{x}/y$, we obtain

$$\dot{\varepsilon} = -1.32\varepsilon^2, \quad (71)$$

which is somewhat weakened with respect to the nonlinear result (37), namely, $\dot{\varepsilon} = -2.22\varepsilon^2$. Notice that the power of the driving term is the same, which shows that no drastic changes are involved in the perpendicular relaxation.

In the limit $\varepsilon \to 0$ (i.e., $x \to 3$, $y \to 0$), using $\sigma(3,0) = 23.61$, the rates become

$$\dot{x} = -366.1, \quad \dot{y} = 99.98, \quad \dot{z} = -83.07. \quad (72)$$

Approximating $\dot{\varepsilon}$ by $\dot{\varepsilon} \approx \dot{y}/x$ we obtain

$$\dot{\varepsilon} = 33.3, \quad (73)$$

which has to be compared with the nonlinear expression (39). Except for very small values of ε for which the logarithmic term dominates, the relaxation is quicker in the test-particle treatment, as seen in Fig. 2.

The absence of $\ln \varepsilon$ in (73), furthermore, proves that this singularity is due to the nonlinearity in the Fokker–Planck operator. Hence anisotropy and nonlinearity are both required to get a singular enhancement of the relaxation speed for $\varepsilon \to 0$.

Finally, we investigate the asymptotic limit $\varepsilon \to 1$, define

$$\xi = x - 1, \quad \eta = y - 1, \quad \zeta = z - \tfrac{3}{2} = \xi/2 + \eta, \quad \delta = |\eta - \xi|, \quad (74)$$

and replace ε by

$$\varepsilon = 1 + \eta - \xi = 1 \pm \delta \quad (\varepsilon \gtrless 1). \quad (75)$$

In the limit $\varepsilon \to 1$, we then obtain from (66),

$$\dot{\xi} = (-3^{1/2}/10)(7\xi - 2\eta), \quad \dot{\eta} = (3^{1/2}/10)(\xi - 6\eta), \quad (76)$$

from which follows

$$\dot{\delta} = (-3^{1/2}/5)4\delta \approx -1.39\delta, \quad (77)$$

$$\dot{\zeta} = (-3^{1/2}/2)\zeta. \quad (78)$$

Not only is the energy not conserved, but also the rate of isotropization is faster in the test-particle treatment, since the nonlinear solution is [see Eq. (33)]

$$\dot{\delta} = (-3^{1/2}/5)\delta \propto -1.039\delta. \quad (79)$$

This gives a factor $\frac{4}{3}$ faster approach to thermal equilibrium, and is independent of the sign of $\varepsilon - 1$.

In conclusion, this section has shown the sensitivity of the relaxation rate to changes in the collision operator in the case of plasmas that are hotter in the parallel direction, whereas no such effect is obtained for perpendicularly heated plasmas.

Two basic questions remain: How large is the effect of neglecting unlike-particle collisions, and how good is the assumption of a bi-Maxwellian adopted in the previous models?

We will first treat the second question and then come back to the first one in Sec. VII.

VI. NUMERICAL STUDY OF TEMPERATURE RELAXATION

A clear answer to how well the bi-Maxwellian shape is maintained can only be given numerically. We have solved the Coulomb relaxation of an initially bi-Maxwellian distribution numerically using a nonlinear Fokker–Planck code. Only like-particle collisions have been taken into account. A similar program has been used by Jorna and Wood,[23] who obtained similar results.

The numerical procedure takes advantage of a collision package developed at Livermore Laboratory.[24,25] Details of the code including the boundary conditions can be found in Ref. 26. In general, seven Legendre polynomials were considered to be sufficient to represent f, g, and h. The discretization in v space uses 50 pitch angle points and 300 speed points. The maximum velocity was chosen to be $15(2T_{\parallel 0}/m)^{1/2}$ for the case $\varepsilon > 1$ and $6(2T_{\parallel 0}/m)^{1/2}$ for $\varepsilon < 1$, where $T_{\parallel 0}$ is the initial parallel temperature. Also the step size in t has been varied to obtain results that are essentially independent of it. Energy was conserved within one percent and density to one part in 10^6.

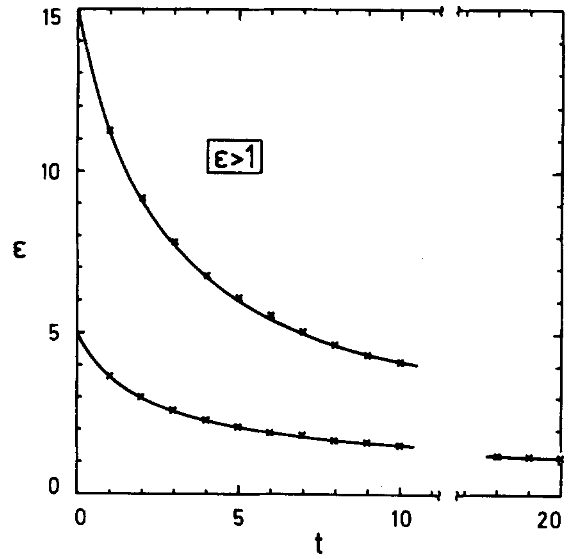

FIG. 5. Comparison between the analytically (solid line) and numerically (crosses) obtained time evolution of ε ($\varepsilon > 1$) for two initial parameters, $\varepsilon(0) = 15$, and $\varepsilon(0) = 5$, respectively.

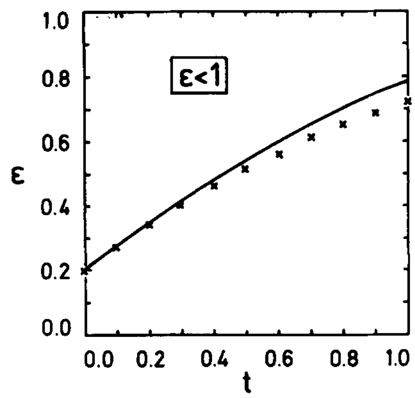

FIG. 7. Like Fig. 5, but for $\varepsilon < 1$.

To measure the departure of f from bi-Maxwellian, the following integrals have been calculated:

$$Q_n^\alpha(t) = \frac{\int_0^\infty dv_\perp\, v_\perp^{n+1} | f_\perp(v_\perp,t) - f_{\perp \mathrm{bM}}(v_\perp,t)|^\alpha}{\int_0^\infty dv_\perp\, v_\perp^{n+1} [f_{\perp \mathrm{bM}}(v_\perp,t)]^\alpha}, \tag{80}$$

$$R_n^\alpha(t) = \frac{\int_{-\infty}^{+\infty} dv_\parallel\, |v_\parallel|^n | f_\parallel(v_\parallel,t) - f_{\parallel \mathrm{bM}}(v_\parallel,t)|^\alpha}{\int_{-\infty}^{+\infty} dv_\parallel\, |v_\parallel|^n [f_{\parallel \mathrm{bM}}(v_\parallel,t)]^\alpha}, \tag{81}$$

where $n = 0$, 1, 2, or 3 and $\alpha = 1$ or 2. The distributions appearing in (80) and (81) are reduced distribution functions (see Sec. IV). The subscript bM refers to bi-Maxwellian with temperatures $T_\perp$ and $T_\parallel$, which are given by the code at time t. In these integrals powers of the velocity and of the deviation of the distribution from bi-Maxwellian appear as weighting factors. The strong decrease of the distribution function at suprathermal velocities implies that moments with $\alpha = 2$, called hereafter the quadratic moments, focus on departures at small speeds, whereas moments with $\alpha = 1$ (the linear moments) emphasize departures in the tail region.

The results are displayed in Figs. 5–8, in which the time t is dimensionless, being normalized this time by $\{[m(2T_{\parallel 0})^3]^{1/2}/4\pi n(Ze)^4 \ln \Lambda\}$, i.e., t differs from τ, introduced in Sec. III by the factor $\frac{1}{4}\sqrt{(\pi/2)[1 + 2\varepsilon(0)]^3}$, which depends on the initial ε.

Figure 5 shows the time evolution of ε for two initial conditions, $\varepsilon(0) = 15$ and $\varepsilon(0) = 5$. The solid line repre-

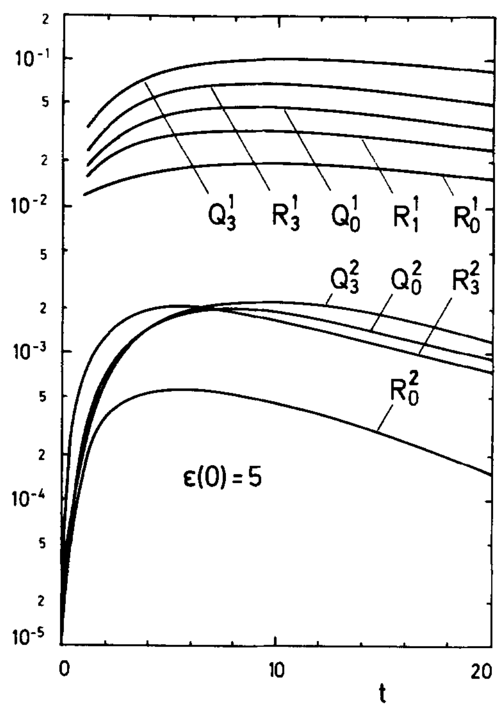

FIG. 6. Some integrals Q_n^α, R_n^α, (80), and (81) as functions of time for the case $\varepsilon(0) = 5$.

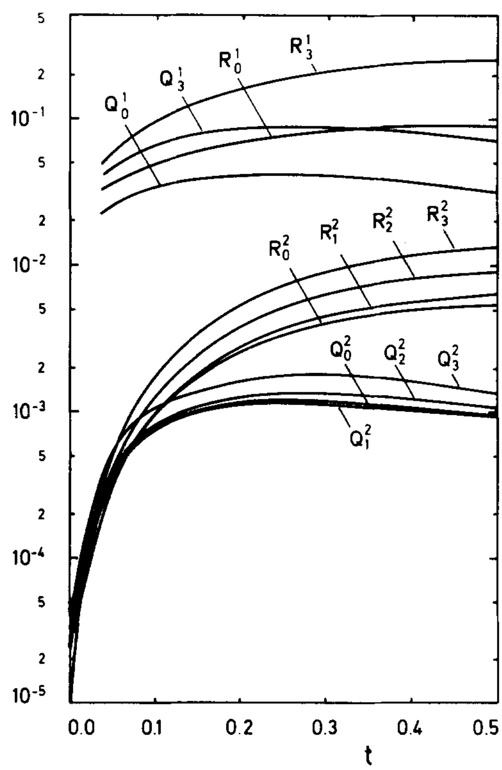

FIG. 8. Some integrals Q_n^α, R_n^α, (80), and (81), as functions of time for the case $\varepsilon(0) = 0.2$.

sents the analytical solution corresponding to (30) in Sec. III, whereas the numerical values of ε obtained by the Fokker–Planck code are marked by crosses.

We find hardly any difference. Only a small deviation of less than 2% is found, the numerical values lying systematically above the analytic ones, indicating a weak slowing down of the evolution. The evolution of ε is therefore remarkably well described at any stage by the analytic theory based on the bi-Maxwellian model. This behavior of the energy relaxation is not obvious, especially if one observes that during the evolution, the bi-Maxwellian shape is strictly not maintained. This is seen in Fig. 6, where several integrals Q^{α}_{n}, R^{α}_{n} are plotted as functions of time for $\varepsilon(0) = 5$. The excitation of these moments reflects the departures from the bi-Maxwellian shape. The latter occur predominantly in the high velocity region since the linear moments are up to two orders of magnitude larger than the quadratic ones. There are two time scales involved, a shorter one in which the distortion builds up and a longer one in which it gradually decays to zero. Maximum excitation has been achieved within the displayed time interval. Moments of higher order in the velocity typically exceed the lower-order ones, e.g., $R^{1}_{m} > R^{1}_{n}$ for $m > n$, as it should for tail deformation. Furthermore, for fixed n and α, a perpendicular moment Q^{α}_{n} exceeds the corresponding parallel moment R^{α}_{n}, as one expects when high energy tails, directed mainly in the perpendicular direction, are involved. The maximum values attained are rather moderate, $|Q^{1}_{n}|,|R^{1}_{n}| \lesssim 10^{-1}$, and the quadratic moments are about two orders of magnitude below this level, indicating weak departures at small speeds.

We therefore conclude that for $T_{\perp}/T_{\parallel} > 1$ the bulk of the distribution and consequently the energy relaxation are fairly accurately modeled by the bi-Maxwellian model.

This is no longer true for the opposite case, $T_{\perp}/T_{\parallel} < 1$. Figure 7 displays $\varepsilon(t)$ for an initial value of $\varepsilon(0) = \frac{1}{5}$. Again, the analytical solution is given by the solid line and the numerical one is marked by crosses. We generally observe a slowing down of the relaxation toward $\varepsilon = 1$. In other words, the parallel relaxation takes place slower than the bi-Maxwellian model would predict. The reason for this deviation can be found by considering the moments Q^{α}_{n},R^{α}_{n}, presented in Fig. 8. Several new features, distinct from those of Fig. 6, are recognized: (i) the parallel moments (R^{α}_{n}) now dominate the perpendicular ones (Q^{α}_{n}), for fixed n and α; (ii) whereas the perpendicular moments have saturated within the given time interval the parallel moments are still increasing, especially the quadratic ones (R^{2}_{n}); (iii) the linear parallel moments exceed the 10^{-1} level, whereas the quadratic ones reach 10^{-2} level, thus being one order of magnitude larger than the corresponding moments in Fig. 6.

These properties together with those in accord with Fig. 6 (e.g., $R^{\alpha}_{m} > R^{\alpha}_{n}$ for $m > n$, two time scales) allow the fo lowing conclusions: The deviation from bi-Maxwellian sei in at high (parallel) velocities and stretches over the cours of time toward bulk velocities affecting at later stages th main body of the distribution. It is this latter property thɛ accounts for the slowing down of the "true" relaxatioı These bulk distortions from bi-Maxwellian coming up i time are essentially the reason for the different behavior (the analytical and numerical $\varepsilon(t)$ observed in Fig. 7.

In conclusion, the bi-Maxwellian model is found to t less accurate in describing the relaxation of an initially b Maxwellian distribution in cases where $T_{\parallel} > T_{\perp}$. Not onl modifications of the collision operator like the one in Sec. \ but also imprecise representations of the distribution, effecı that are obviously correlated, have an influence on the rela› ation of distributions stretched in the $v_{\parallel}$ direction.

On the other hand, the two-dimensional geometry i perpendicularly heated plasma minimizes these effects, s that the error introduced by modifications of the collisio operator and by changes of the distribution shape from b Maxwellian can be ignored.

The last point we want to investigate is the influence (unlike-particle collisions neglected so far.

VII. UNLIKE-PARTICLE COLLISIONS WITHIN THE BI-MAXWELLIAN MODEL

In this section we take account of the sum over differeı species introduced in Sec. II and assume that species a repr sents the anisotropic relaxing component and species $b \neq$ stands for the other already relaxed isotropic component assuming $T_b = T_{\infty}$. The contribution of unlike-partic collisions is then given by the coefficients (19)–(21). Worl ing first within the test-particle approach, and using similɛ integration techniques to those in Sec. V, we obtain

$$\dot{x} = 3\left(\frac{3}{2}\right)^{1/2} \frac{1}{(x-y)} \sum_b \omega \left(\frac{\mu + (3+2\mu)x}{(\mu+x)^{1/2}} - [\mu + 2(1+\mu)x + y]\sigma_{\mu}(x,y)\right), \quad (82\text{;}$$

$$\dot{y} = -\left(\frac{3}{2}\right)^{3/2} \frac{1}{(x-y)} \times\left(\sum_b \omega \frac{(\mu+x)^{1/2}[\mu + (3+2\mu)y]}{(\mu+y)} - [\mu + 2x + (1+2\mu)y]\sigma_{\mu}(x,y)\right), \quad (82\text{l}$$

$$\dot{z} = 3\left(\frac{3}{2}\right)^{1/2} \sum_b \omega\mu \left(\frac{1+\mu}{(\mu+x)^{1/2}(\mu+y)} - \sigma_{\mu}(x,y)\right), \quad (82\text{,}$$

where we have defined

$$\sigma_{\mu}(x,y) = \begin{cases} [1/(y-x)^{1/2}]\tan^{-1}[(y-x)/(\mu+x)]^{1/2}, & y \geqslant x, \\ [1/(x-y)^{1/2}]\tanh^{-1}[(x-y)/(\mu+x)]^{1/2}, & x \geqslant y, \end{cases} \quad (8\text{:}$$

$$\mu = m_a/m_b, \quad \omega = (n_b/n_a)(Z_b/Z_a)^2. \quad (8\text{4}$$

The sum in (82) includes the self-collision term $b = a$. It is easily seen that the old result (66) is obtained when only self-collisions are considered. The function $\sigma_{\mu}(x,y)$ is ɛ extension of $\sigma(x,y)$, defined in (68), and reduces to that the limit $\mu \to 1$. On the other hand, treating self-collisions nonlinearly, as presented in Sec. III, the term $b = a$ in each equation (82) has to be replaced by the corresponding nonlinear expression. Making use of

$$\frac{dW_\parallel}{d\tau} = \frac{-nT_\parallel}{(1+2\varepsilon)}\frac{d\varepsilon}{d\tau} \tag{85}$$

and of (30), we obtain

$$\dot{x} = -(x/2)[(1+2\varepsilon)^{3/2}/(1-\varepsilon)] \times [(2+\varepsilon)g(\varepsilon) - 3] + X_R, \tag{86a}$$

$$\dot{y} = (x/4)[(1+2\varepsilon)^{3/2}/(1-\varepsilon)] \times [(2+\varepsilon)g(\varepsilon) - 3] + Y_R, \tag{86b}$$

$$\dot{z} = Z_R, \tag{86c}$$

where $g(\varepsilon)$ is defined in (31) and X_R, Y_R, and Z_R are given by the corresponding rhs of Eqs. (82a)–(82c) without the self-collision term $b = a$.

Both sets of equations, (82) and (86), can now be used to estimate the effect of unlike-particle collisions in a simple plasma consisting of electrons and Z-fold charged ions.

First we treat the electron relaxation: $a = e$, $b = i$, $\mu = m_e/m_i \ll 1$, $n_e = Zn_i$. To lowest order in μ we find

$$X_R = Z\,3(\tfrac{3}{2})^{1/2}[1/(x-y)][3x^{1/2} - (2x+y)\sigma_0(x,y)], \tag{87a}$$

$$Y_R = -Z(\tfrac{3}{2})^{3/2}[1/(x-y)][3x^{1/2} - (2x+y)\sigma_0(x,y)], \tag{87b}$$

$$Z_R = 0, \tag{87c}$$

where $\sigma_0(x,y)$ follows from (83) by setting $\mu = 0$. Two conclusions can be drawn immediately: (i) the unlike-collision terms, being proportional to Z, contribute in the lowest order to the time evolution of the electron temperatures $T_\parallel$ and $T_\perp$, the contribution becoming stronger the higher Z; and (ii) the time development of the total energy is not affected to lowest order in μ.

Hence e–i collisions influence the isotropization of anisotropic electrons and have to be taken into account in a more complete treatment of the isotropization process.

Second, we deal with the relaxation of ions and set $a = i$, $b = e$, $\mu = m_i/m_e \gg 1$, and $(Z_e/Z_i)^2 n_e/n_i = Z^{-1}$. It is found by Taylor expansion of the e–i collision terms with respect to μ^{-1} that X_R, Y_R, and Z_R are proportional to $Z^{-1}\mu^{-1/2}$. Therefore the e–i collisions only weakly influence the Maxwellization process of the ions.

In a simple plasma, the ion energy relaxation is determined by ion self-interactions only.

In fully ionized plasmas, with several ion species, however, such as in fusion plasmas, the relaxation of a given ion species will generally be affected by the presence of the other ion components, as μ is of order unity. The unlike-collision terms are then no longer small in comparison with the self-interaction terms.

Comparing the involved time scales we find that the ions isotropize by a factor of

$$\nu_{Ei}/\nu_{Ee} = (m_e/m_i)^{1/2}Z^3$$

slower than the electrons. The energy exchange between them takes place at a still slower rate,

$$\nu_{Ei}/\nu_{Ee} = (m_e/m_i)Z,$$

justifying the neglect of time change of the isotropic temperature of the unlike species. These time scales basically agree with those of Spitzer and others.[7]

In conclusion, the temperature relaxation of electrons appears to be affected by unlike-particle collisions, whereas only self-interactions account for the isotropization process of ions in simple plasmas.

VIII. SUMMARY AND CONCLUSIONS

In concluding this paper, we point out that the above results presumed distributions that are close to bi-Maxwellian shape, for example, egg shaped. Even if a distorted distribution as a whole does not come close to this requirement one often finds that it can be split into a isotropic cold part and an anisotropic hot one. If the latter can be approximated by a bi-Maxwellian distribution, if necessary by including a drift, the above results, in which the cold isotropic particles then act as field particles, are applicable. For distributions not satisfying this criterion one has to resort to numerical solutions of the Fokker–Planck equation.

For numerical purposes the following conclusions can be drawn from the present paper.

(i) In cases where the distribution is mainly distorted in the direction perpendicular to the magnetic field, such as in cyclotron resonance absorption of rf waves or perpendicular injection of neutral particles, the numerical effort can be reduced without loss of accuracy by using simplified, and hence more time efficient, codes based on the test-particle approach.

(ii) In cases of parallel injection and/or distributions distorted mainly in the direction of the magnetic field, however, a nonlinear Fokker–Planck code[23–26] is usually called for.

These conclusions rest on our observation that the temperature relaxation is insensitive to changes in the collision operator and to distortions from bi-Maxwellian in the case of "perpendicular" relaxation, $T_\perp/T_\parallel > 1$, only, whereas for "parallel" relaxation such an independence was not found.

ACKNOWLEDGMENTS

H. Schamel wishes to thank the JET Theory Division for their kind hospitality during his stay.

[1]N. J. Fisch, Rev. Mod. Phys. **59**, 175 (1987).
[2]S. Livi, E. Marsch, and H.Rosenbauer, J. Geophys. Res. **91**, 8045 (1986).
[3]S. Chandrasekhar, Rev. Mod. Phys. **15**, 1 (1943).
[4]L. Spitzer Jr., *Physics of Fully Ionized Gases* (Interscience, New York, 1962), 2nd ed.
[5]B. A. Trubnikov, in *Reviews of Plasma Physics*, Vol. 1, edited by M. A. Leontovich (Consultants Bureau, New York, 1965), p. 105.
[6]T. H. Stix, Nucl. Fusion **15**, 737 (1975).
[7]F. L. Hinton, in *Handbook of Plasma Physics*, Basic Plasma Physics I, edited by M. N. Rosenbluth and R. Z. Sagdeev (North-Holland, Amsterdam, 1983), Vol. I, p. 147.
[8]V. I. Kogan, *Plasma Physics and the Problem of Controlled Thermonuclear Reactions* (Pergamon, New York, 1961), Vol. I, p. 153.
[9]G. Lehner, Z. Phys. **206**, 284 (1967).
[10]R. Chodura and F. Pohl, Plasma Phys. **13**, 645 (1971).
[11]A. R. Barakat and R. W. Schunk, Plasma Phys. **24**, 389 (1982).
[12]L. Landau, Phys. Z. Sowjetunion **10**, 154 (1936).

[13]M. N. Rosenbluth, W. MacDonald, and D. Judd, Phys. Rev. **107**, 1 (1957).
[14]N. Rostoker, Phys. Fluids **3**, 922 (1960).
[15]S. Ichimaru and M. N. Rosenbluth, Phys. Fluids **13**, 2778 (1970).
[16]K. Matsuda, Phys. Fluids **26**, 1508 (1983).
[17]D. Montgomery, G. Joyce, and L. Turner, Phys. Fluids **17**, 2201 (1975).
[18]P. Ghendrih, A. Samain, and J. H. Misguich, Phys. Lett. A **119**, 354 (1987).
[19]H. E. Mynick, J. Plasma Phys. **39**, 303 (1988).
[20]A. B. Mikhailovskii, in *Theory of Plasma Instabilities* (Consultants Bureau, New York, 1974), Vol. I, Chaps. 10 and 15.
[21]M. Abramowitz and J. A. Stegun, *Handbook of Mathematical Functions* (Dover, New York, 1965).
[22]O. D. Kellog, *Foundations of Potential Theory* (Ungar, New York, 1929).
[23]S. Jorna and L. Wood (private communication).
[24]M. G. McCoy, A. A. Mirin, and J. Killeen, Comput. Phys. Commun. **24**, 37 (1981).
[25]J. Killeen, G. D. Kerbel, M. G. McCoy and A. A. Mirin, *Computational Methods for Kinetic Models of Magnetically Confined Plasmas*, Springer Series in Computational Physics (Springer, New York, 1986).
[26]M. R. O'Brien, M. Cox, and D. F. H. Start, Comput. Phys. Commun. **40**, 123 (1986).